Computers and Concrete, *Vol. 24, No. 6 (2019) 499-511*
DOI: https://doi.org/10.12989/cac.2019.24.6.499

Double bonded Cooper-Naghdi micro sandwich cylindrical shells with porous core and CNTRC face sheets: Wave propagation solution

Raziye Yazdani and Mehdi Mohammadimehr*

Department of Solid Mechanics, Faculty of Mechanical Engineering, University of Kashan, P.O. Box: 87317-53153, Kashan, Iran

(*Received August 29, 2019, Revised October 21, 2019, Accepted October 22, 2019*)

Abstract. In this paper, wave propagation of double-bonded Cooper-Naghdi micro sandwich cylindrical shells with porous core and carbon nanotube reinforced composite (CNTRC) face sheets are investigated subjected to multi-physical loadings with temperature dependent material properties. The governing equations of motion are derived by Hamilton's principle. Then, the influences of various parameters such as wave number, CNT volume fraction, temperature change, Skempton coefficient, material length scale parameter, porosity coefficient on the phase velocity of double-bonded micro sandwich shell are taken into account. It is seen that by increasing of Skempton coefficient, the phase velocity decreases for higher wave number and the results become approximately the constant. Also, by increasing of the material length scale parameter, the cut of frequency increases, because the stiffness of micro structure increases. The obtained results for this article can be used to detect, locate and quantify crack.

Keywords: wave propagation; double-bonded Cooper-Naghdi micro sandwich cylindrical shells; porous core; CNTRC; multi-physical loadings

1. Introduction

One the most application of wave propagation is that it can be presented to detect, locate and quantify crack, thermal debond, and corrosion damage in a solid structure and a sandwich honeycomb thermal protection panel (Doyle 1997, Ghorbanpour-Arani *et al*. 2017, 2018). A wave propagation can identify small defects because propagating waves typically consist of small wavelengths. Some researchers worked about wave propagation of beam, plate and shell in macro, micro and nano scales, for example, Hosseini *et al*. (2013) presented a parametric study on the numerical simulation of Lamb wave propagation in metallic foam sandwich structures. In the other work, they (2013) introduced a new non-reflecting boundary condition using dashpot elements that becomes an useful tool to efficiently simulate Lamb wave propagation within composite structures, such as honeycomb and composite fiber reinforced plate. Sorokin and Grishina (2004) studied propagation of flexural and shear waves in an unbounded sandwich beam that is considered as a 'unit width strip'.

Based on Mindlin plate and Kirchhoff plate theories, Xu and Deng (2016) considered the wave propagation characteristics in thick conventional and auxetic cellular structures, that the effects of negative Poisson's ratio, shear factor and orthotropic mechanical properties on the dynamic behaviors of thick plates are investigated. Sellappan *et al*. (2015) demonstrated wave propagation through alumina-porous laminates. They considered high-speed imaging and transmitted force measurements to gain an insight into stress wave propagation and mitigation through such a layered system and introduced uniformly distributed porosities. Narendar and Gopalakrishnan (2012) illustrated a study of terahertz wave propagation properties in nanoplates with surface and small-scale effects. They concluded that in macroscopic and even microscopic structural elements, surface effects can be neglected and classical theories are sufficient and also as the structural size decreases towards the nanoscale regime, the surface-to-bulk energy ratio increases and surface effects must be considered. Farahani and Barati (2015) presented vibration analysis of functionally graded cylindrical shell submerged in an incompressible fluid. Using the wave propagation approach and Flügge shell equations, they established the axial and lateral hydrostatic pressure based on first order shear deformation theory of shell motion. Kakar (2015) presented SH-wave propagation in a heterogeneous layer over an inhomogeneous isotropic elastic half-space.

Some researchers have been investigated plane problem of interaction between an elastic longitudinal wave and a cylindrical shell with axial cut (Porokhovs'kyi 2009), wave propagation in an elastic structure by modeling a split Hopkinson pressure bar (Netrebko 2013), wave propagation in functionally graded- carbon nanotubes (FG-CNT)-reinforced piezoelectric composite micro plates (Arani *et al*. 2016), stress wave propagation in a rectangular bar (Rasulova and Shamilova 2016), wave propagation analysis of twisted micro-beam (Mohammadimehr *et al*. 2016a), plane acoustic wave propagation through a composite of elastic (Shamaev *et al*. 2017), localized strain waves in a nonlinearly elastic conducting medium interacting with a magnetic field (Erofeev *et al*. 2017), wave propagation analysis of sandwich nano-beam (Ghorbanpour Arani *et al*.

*Corresponding author, Associate Professor
E-mail: mmohammadimehr@kashanu.ac.ir

Copyright © 2019 Techno-Press, Ltd.
http://www.techno-press.org/?journal=cac&subpage=8
ISSN: 1598-8198 (Print), 1598-818X (Online)

2017), wave propagation behavior of coupled viscoelastic micro plates (Jamali *et al*. 2017), plane wave propagation in an elastic anisotropic media (Rozhkova 2018).

In the recent years, cylindrical shells are one of the most used parts in various industries. They are used in gas turbines, rotary kilns, aircrafts, spacecraft, tankers, pipelines and so on. For proper design, strength to weight ratio of shell should be as high as possible for material consumption and optimal cost reductions. Hence, composite and sandwich structures have been used to achieve this goal. Murmu *et al*. (2012) studied the mechanical behavior of double-walled carbon nanotube (DWCNT) under a magnetic field for nonlocal transverse vibration. They found that the natural frequencies of the system increase in the presence of a magnetic field. Ansari *et al*. (2011) extended first-order shear deformation theory (FSDT) for functionally graded materials (FGMs) nanoshell vibration. They indicated that increasing the length to thickness ratio of micro beams leads to decrease the natural frequency. Ke *et al*. (2015) illustrated the free vibration of nonlocal piezoelectric nanoplates under various boundary conditions. They used the nonlocal elasticity theory and Hamilton's principle to derive the governing equations. They proved that the electrical voltage for simply supported boundary conditions doesn't have a significant effect on the mode shape of vibration motions, while the effects of this variable on the clamped boundary conditions is considerable. Li and Pan (2015) predicted the static behavior and vibrations of the piezoelectric microplate made of FGMs based on the modified coupling stress theory. They illustrated that the amount of electrical displacement and the stresses increases with increasing of electric loading. Some researchers worked about nonlinear dynamic analysis (Duc 2013, 2016, 2019, Mohammadimehr *et al*. 2017b), nonlinear buckling analysis (Cong *et al*. 2018, Khoa *et al*. 2019, Ghorbanpour Arani *et al*. 2016, Mohammadimehr *et al*. 2016c), vibration analysis (Duc and Cong 2018, Mohammadimehr *et al*. 2017a, 2018), nonlinear static and vibration analysis using FEM (Mohammadimehr and Alimirzaei 2016), nonlinear wave propagation (Shariyat *et al*. 2019).

Tornabene (2009) considered vibration analysis of functionally graded conical, cylindrical shell and annular plate structures with a four-parameter power-law distribution. Duc *et al*. (2015) studied mechanical and thermal stability of eccentrically stiffened functionally graded conical shell panels resting on elastic foundations and in thermal environment. Pourasghar and Kamarian (2016) obtained thermo-elastic response of carbon nanotubes (CNT) reinforced cylindrical panel resting on elastic foundation using elasticity theory with temperature-dependent materials. Mohammadimehr *et al*. (2016b) investigated free vibration behaviors of microcomposite plate reinforced by functionally graded single-walled carbon nanotube (FG-SWCNT) under hydro-thermal environments using third-order shear deformation theory (TSDT) and modified strain gradient theory (MSGT). Do *et al*. (2017) considered analysis of bi-directional functionally graded plates by FEM and a new third-order shear deformation plate theory. Zghal *et al*. (2018) presented the buckling analysis of functionally graded power-based and carbon nanotubes-reinforced composite plates and curved panels. Saidi *et al*. (2019) studied the vibration and stability analysis of porous plates reinforced by graphene platelets under aerodynamical loading. The high-order free vibration analysis of two type sandwich beams including CNTs reinforced nanocomposite face sheets and different core is studied by Mohammadimehr and shahedi (2016). They concluded that the irst natural frequency decreases with increasing of temperature change. Frikha *et al*. (2018) investigated the dynamic analysis of functionally graded carbon nanotubes-reinforced plate and shell structures using a double directors finite shell element. Moradi-Dastjerdi and co-workers (2019) considered the dynamic behavior of nanocomposite sandwich plates subjected to periodic thermo-mechanical loadings. Tornabene *et al*. (2011) illustrated free vibration analysis of FGM and laminated doubly curved shells and panels of revolution with a free-form meridian. Mohammadimehr and Mostafavifar (2016) studied the free vibration of temperature-dependent sandwich plate with FG-CNTs reinforced nanocomposite face sheets under magnetic field. They proved that increasing of the aspect ratio and magnetic field leads to increase in the dimensionless natural frequency while it decreases by rising of the temperature change. Tornabene *et al*. (2015) presented stress and strain recovery for functionally graded free-form and doubly-curved sandwich shells using higher-order equivalent single layer theory. Mohammadimehr *et al*. (2017c) presented the vibration analysis of double-bonded sandwich microplates with nanocomposite facesheets reinforced by symmetric and un-symmetric distributions of nanotubes under multi physical fields. Sobhy and Zenkour (2018) illustrated the effect of magnetic field on thermo-mechanical buckling and vibration analysis of viscoelastic sandwich nanobeams with CNT reinforced face sheets on a viscoelastic substrate. Al-Kamal (2019) presented nominal axial and flexural strengths of high-strength concrete columns. Parate and Kumar (2019) considered shear strength model for reinforced concrete beam-column joints based on hybrid approach. Wu *et al*. (2019) studied experimental study on shear damage and lateral stiffness of transfer column in SRC-RC hybrid structure. Rajabi and Mohammadimehr (2019) depicted bending analysis of a micro sandwich skew plate using extended Kantorovich method based on Eshelby-Mori-Tanaka approach.

In this paper, wave propagation of double-bonded Cooper-Naghdi micro sandwich cylindrical shells with saturated porous core and carbon nanotube reinforced composite (CNTRC) face sheets are investigated subjected to multi-physical loadings such as magneto-hydro-thermo-mechanical loadings with temperature dependent material properties. The governing equations of motion are derived by Hamilton's principle.

2. Geometry and simulation

Consider micro sandwich cylindrical shell with saturated porous core and carbon nanotube reinforced composite (CNTRC) face sheets subjected to multi-physical

Table 1 Efficiency coefficients of NTs (Ghorbanpour Arani *et al*. 2016)

V_{NT}^*	η_1	η_2	η_3
0.11	0.149	0.934	0.934
0.14	0.150	0.941	0.941
0.17	0.149	1.381	1.381

Table 2 Material properties depended on temperature for (10, 10) SWCNT (R=0.68 nm, L=9.2 6nm, h=0.067 nm, ρ=1400 Kg/m^3, ν_{12}=0.175) (Farajpour *et al*. 2016)

Temperature (K)	E_{11}^{CNT} (TPa)	E_{22}^{CNT} (TPa)	G_{12}^{CNT} (TPa)	α_{11}^{CNT} (1/GPa.K)	α_{22}^{CNT} (1/GPa.K)
300	5.6466	7.08	1.9445	3.4584	5.1682
500	5.5308	6.9348	1.9643	4.5361	5.0189
700	5.4744	6.8641	1.9644	4.6677	4.8943

Table 3 The mechanical and electrical properties for CNT and BNNT as reinforced in face sheets

All constants	The values of parameters
Elastic cons tan*ts* (*CNT*)	C_{11}=5.8249 TPa, C_{12}=1.01937 TPa, C_{22}=7.3037 TPa, C_{44}=C_{55}=C_{66}=1.9445 TPa, υ=0.175, V_{CNT}=0.17
Elastic cons tan*ts* (*BNNTs*)	C_{11}=C_{22}=C_{33}=2.035 TPa, C_{12}=C_{13}=C_{23}=0.692 TPa, C_{44}=C_{55}=C_{66}=0.672 TPa, υ=0.34, V_{NT}=0.17
Piezoelectric cons tan*ts* (*BNNT*)	e_{31}=0.95 C/m^2, e_{32}=−0.45 C/m^2, e_{24}=−0.276 C/m^2, e_{15}=−0.009 C/m^2
Dielectric cons tan*ts*	K_{11}=K_{22}=K_{33}=1.7708×10^{-10}

loadings with Length L, thickness h and inner radius R of the micro sandwich cylindrical shell. Also, h_c, h_b and h_t are the thicknesses of core, and face sheets, respectively. The micro sandwich cylindrical shell with temperature dependent material properties is embedded by Pasternak foundation with K_{wi} and K_{Gi}, i=1,2,3. The micro sandwich cylindrical shell is subjected to applied voltage ψ_0 and magnetic field φ_0.

Displacement fields of the micro sandwich moderately cylindrical shell based on Cooper-Naghdi theory are given by

$$\begin{aligned} U_x(x,\theta,z,t) &= u(x,\theta,t) + z\,\beta_x(x,\theta,t) \\ U_\theta(x,\theta,z,t) &= v(x,\theta,t) + z\,\beta_\theta(x,\theta,t) \\ U_z(x,\theta,z,t) &= w(x,\theta,t) \end{aligned} \tag{1}$$

where, $u(x,\theta,t)$, $v(x,\theta,t)$, $w(x,\theta,t)$, $\beta_x(x,\theta,t)$ and $\beta_\theta(x,\theta,t)$ are middle surface displacements and rotations in the longitudes, peripheral and thickness direction of the micro sandwich moderately cylindrical shell, respectively.

Strain-displacement relations for each of face sheet and core can be expressed in Appendix A.

The various porous distribution types along thickness for core, the extended mixture approach is used for effective material properties of face sheets, and the material properties of nanotubes (NTs) are shown in Appendix B.

Tables 1 and 2 show the efficiency coefficients of nanotubes (NTs) and the material properties depended on temperature for (10, 10) SWCNT (R=0.68 nm, L=9.26 nm, h=0.067 nm, ρ=1400 Kg/m^3, ν_{12}=0.175), respectively. Also, the mechanical and electrical properties for face sheets reinforced by nanotubes (NTs) is depicted in Table 3.

Table 4 The properties of matrix materials for face sheet layers ($BiTiO_3$−$CoFe_2O_4$)

All constants	The values of parameters
Elastic constants	C_{11}=C_{22}=226 MPa, C_{12}=125 MPa, C_{13}=124 MPa, C_{33}=216 MPa, C_{44}=C_{55}=44.2 MPa, C_{66}=50.5 MPa
Piezoelectric constants	e_{31}=e_{32}=−2.2 C/m^2, e_{15}=e_{24}=5.8 C/m^2, e_{33}=9.3 C/m^2
Piezomagnetic constants	q_{31}=q_{32}=290.1 H/m, q_{15}=q_{24}=275 H/m, q_{33}=349.9 H/m
Dielectric constants	K_{11}=K_{22}=5.64×10^{-9}, K_{33}=6.35×10^{-9}
Magnetoelectric constants	g_{11}=g_{22}=5.367×10^{-12} V/m.Oe, g_{33}=2737.5×10^{-12} V/m.Oe
Magnetic constants	μ_{11}=μ_{22}=−297×10^{-6} N/A^2, μ_{33}=53.5×10^{-6} N/A^2
Other constants	ρ=5550 kg/m^3, α=4.74e−5 1/K, ν=0.25, h=2 μm, 1=17.6 μm, L=20 h, K_W=600 GN/m^3, K_G=1000 N/m

The properties of matrix materials for face sheet layers ($BiTiO_3$−$CoFe_2O_4$) is considered in Table 4.

Density, Poison's ratios, thermal and hydro properties of face sheets are written as

$$\begin{aligned} \rho &= \rho_{NT}V_{NT} + \rho_m V_m \\ \nu_{12} &= \nu_{12}^{NT}V_{NT} + \nu_m V_m \\ \alpha_{11} &= \alpha_{11}^{NT}V_{NT} + \alpha_m V_m \\ \alpha_{22} &= (1+\nu_{12}^{NT})\alpha_{22}^{NT}V_{NT} + (1+\nu_m)\alpha_m V_m - \nu_{12}\alpha_{11} \\ \beta_{11} &= \beta_{11}^{NT}V_{NT} + \beta_m V_m \\ \beta_{22} &= (1+\nu_{12}^{NT})\beta_{22}^{NT}V_{NT} + (1+\nu_m)\beta_m V_m - \nu_{12}\beta_{11} \end{aligned} \tag{2}$$

The face sheets are reinforced by NTs. The volume fraction of NTs, V_{NT} for the top and the bottom of face sheets are as

$$\begin{aligned} V_{NT} &= 2\left(\frac{t_1 - z}{t_1 - t_0}\right)V_{NT}^* \text{ for top facesheet} \\ V_{NT} &= 2\left(\frac{z - t_2}{t_3 - t_2}\right)V_{NT}^* \text{ for bottom facesheet} \end{aligned} \tag{3}$$

Using Tables 3 and 4, the equal properties for face sheets can be obtained as follows

$$\begin{aligned} c_{11} &= \frac{c_{11}^{SWNT}c_{11}^{m}}{V_{SWNT}c_{11}^{m} + (1-V_{SWNT})c_{66}^{m}} \\ c_{12} &= c_{11}\left(\frac{V_{SWNT}c_{12}^{SWNT}}{c_{11}^{SWNT}} + (1-V_{SWNT})\frac{c_{12}^{m}}{c_{11}^{m}}\right) \\ c_{22} &= V_{SWNT}c_{22}^{SWNT} + (1-V_{SWNT})c_{22}^{m} \\ c_{66} &= \frac{c_{66}^{SWNT}c_{66}^{m}}{V_{SWNT}c_{66}^{SWNT} + (1-V_{SWNT})c_{66}^{m}} \end{aligned} \tag{4}$$

$$
\begin{aligned}
e_{24} &= V_{SWNT} e_{24}^{SWNT} + (1-V_{SWNT}) e_{24}^{m} \\
e_{32} &= V_{SWNT} e_{32}^{SWNT} + (1-V_{SWNT}) e_{32}^{m} \\
e_{31} &= q_{11}\left(\left(\frac{(1-V_{SWNT}) e_{31}^{SWNT}}{q_{11}^{SWNT}}\right) + \left(\frac{V_{SWNT} e_{31}^{m}}{q_{11}^{m}}\right)\right) \\
e_{15} &= \frac{e_{15}^{m} e_{15}^{SWNT}}{V_{SWNT} e_{15}^{m} + (1-V_{SWNT}) e_{15}^{SWNT}}
\end{aligned}
\tag{5}
$$

$$
\begin{aligned}
K_{11} &= (1-V_{SWNT}) K_{11}^{m} + V_{SWNT} K_{11}^{SWNT} \\
K_{22} &= (1-V_{SWNT}) K_{22}^{m} + V_{SWNT} K_{22}^{SWNT} \\
K_{33} &= (1-V_{SWNT}) K_{33}^{m} + V_{SWNT} K_{33}^{SWNT}
\end{aligned}
\tag{6}
$$

Hamilton's principle can be stated as follows

$$
\int_0^t (\delta T - \delta U - \delta W) dt = 0 \tag{7}
$$

where δU, δW, and δT are the variations of strain energy, work done by external force and kinetic energy, respectively.

The variation of strain energy for three layers of the micro sandwich moderately cylindrical shell based on modified couple stress theory can be written as follows

$$
\begin{aligned}
\delta U = &\int_{-\frac{h_c}{2}-h_b}^{-\frac{h_c}{2}} (\sigma_{ij}\delta\varepsilon_{ij} + m_{ij}\delta\chi_{ij} - D_i\delta E_i - B_i\delta H_i) dV \\
&+ \int_{-\frac{h_c}{2}}^{-\frac{h_c}{2}} (\sigma_{ij}\delta\varepsilon_{ij} + m_{ij}\delta\chi_{ij}) dV \\
&+ \int_{\frac{h_c}{2}}^{\frac{h_c}{2}+h_t} (\sigma_{ij}\delta\varepsilon_{ij} + m_{ij}\delta\chi_{ij} - D_i\delta E_i - B_i\delta H_i) dV
\end{aligned}
\tag{8}
$$

where the stress tensor σ_{ij}, symmetric stress tensor m_{ij} and symmetric rotation gradient tensor are defined.

Electrical and magnetic potential functions can be expressed as

$$
\begin{aligned}
\psi(x,\theta,z,t) &= \frac{2\tilde{z}}{h_p}\psi_0 - \psi(x,\theta,t)\cos\left(\frac{\pi\tilde{z}}{h_p}\right) \\
\varphi(x,\theta,z,t) &= \frac{2\tilde{z}}{h_p}\varphi_0 - \varphi(x,\theta,t)\cos\left(\frac{\pi\tilde{z}}{h_p}\right) \\
\tilde{z} &= z - \frac{h_c}{2} - \frac{h_t}{2}
\end{aligned}
\tag{9}
$$

The variation of kinetic energy is given by

$$
\begin{aligned}
\int_\Omega \delta T &= \int_{-\frac{h_c}{2}-h_b}^{\frac{h_c}{2}+h_t} \delta T + \int_{-\frac{h_c}{2}-h_b}^{\frac{h_c}{2}+h_t} \delta T + \int_{\frac{h_c}{2}}^{\frac{h_c}{2}+h_t} \delta T \\
\delta T &= \int_\Omega \rho(z)\Big[\frac{\partial U_x}{\partial t}\delta\left(\frac{\partial U_x}{\partial t}\right) + \frac{\partial U_\theta}{\partial t} \\
&\quad \delta\left(\frac{\partial U_\theta}{\partial t}\right) + \frac{\partial U_z}{\partial t}\delta\left(\frac{\partial U_z}{\partial t}\right)\Big] dV
\end{aligned}
\tag{10}
$$

$$
\begin{aligned}
\delta T = &\int_\Omega \rho(z)\Big[\left(\frac{\partial u}{\partial t} + z\frac{\partial \beta_x}{\partial t}\right)\delta\left(\frac{\partial u}{\partial t} + z\frac{\partial \beta_x}{\partial t}\right) \\
&+ \left(\frac{\partial v}{\partial t} + z\frac{\partial \beta_\theta}{\partial t}\right)\delta\left(\frac{\partial v}{\partial t} + z\frac{\partial \beta_\theta}{\partial t}\right) + \left(\frac{\partial w}{\partial t}\right)\delta\left(\frac{\partial w}{\partial t}\right)\Big] dx\, d\theta\, dz
\end{aligned}
$$

Variation of kinetic energy must be extended for three layers of the micro sandwich cylindrical shell. Variation of work done by foundation forces for double bonded micro sandwich cylindrical shells can be written as follows

$$
\begin{aligned}
\delta W &= \int_A F^{elastic} \delta w dA \\
F^{elastic_1} &= K_{w1} w_1 - K_{w2}(w_2 - w_1) - K_{G1}\nabla^2 w_1 + K_{G2}\nabla^2 (w_2 - w_1) \\
F^{elastic_2} &= K_{w2}(w_2 - w_1) - K_{G2}\nabla^2 (w_2 - w_1) + K_{w3} w_2 - K_{G3}\nabla^2 w_2
\end{aligned}
\tag{11}
$$

The governing equations of motion by substituting Eqs. (8), (10) and (11) into Eq. (7) are derived that is shown in Appendix C.

3. Solving method

Navier's type solution is considered for the micro sandwich cylindrical shell as follows

$$
\begin{aligned}
u(x,\theta,t) &= U_m e^{i(kx+n\theta+\omega t)} \\
v(x,\theta,t) &= V_m e^{i(kx+n\theta+\omega t)} \\
w(x,\theta,t) &= W_m e^{i(kx+n\theta+\omega t)} \\
\beta_x(x,\theta,t) &= \beta_x e^{i(kx+n\theta+\omega t)} \\
\beta_t(x,\theta,t) &= \beta_t e^{i(kx+n\theta+\omega t)} \\
\varphi(x,\theta,t) &= \varphi_m e^{i(kx+n\theta+\omega t)} \\
\psi(x,\theta,t) &= \psi_m e^{i(kx+n\theta+\omega t)}
\end{aligned}
\tag{12}
$$

where k and n are half axial and peripheral wave numbers, respectively.

In the matrix form

$$
\begin{aligned}
&\{[K] - [M]\omega^2\}\{U\} = 0 \\
&\{U\} = \{U_m \quad V_m \quad W_m \quad \beta_x \quad \beta_t \quad \varphi_m \quad \psi_m\}^T
\end{aligned}
\tag{13}
$$

where $[K]$, $[M]$ and $\{U\}$ are stiffness matrix, mass matrix and displacement vector, respectively.

4. Numerical result and discussion

In this article, wave propagation analysis of double-bonded Cooper-Naghdi micro sandwich cylindrical shells with porous core and carbon nanotube reinforced composite (CNTRC) face sheets are investigated subjected to multi-physical loadings with temperature dependent material properties. The governing equations of motion are derived by Hamilton's principle.

Fig. 1 shows the influence of n for double-bonded micro sandwich shell with composite facesheets reinforced by nanotubes and porous core on the phase velocity and dimensionless wavenumber. It is seen that with increasing n in lower dimensionless wavenumber, the difference

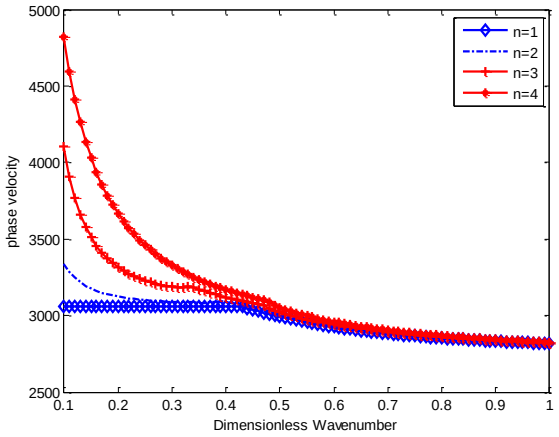

Fig. 1 The influence of *n* for double-bonded micro sandwich shell with composite facesheets reinforced by nanotubes and porous core on the phase velocity

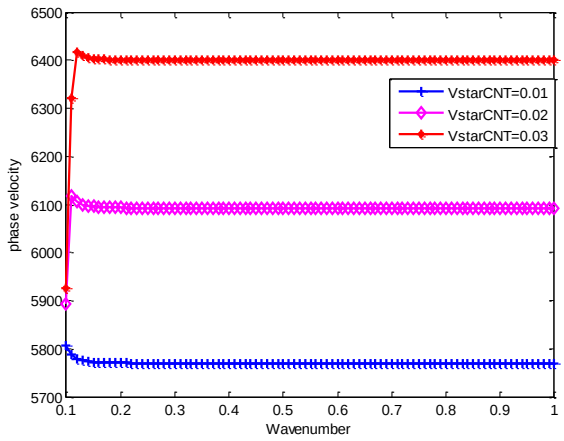

Fig. 2 The influence of various volume fraction on the phase velocity

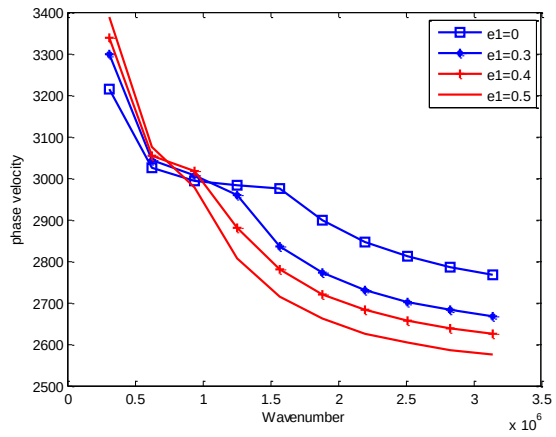

Fig. 3 The influence of porosity coefficient on the phase velocity

between curves for phase velocity increases; while for higher dimensionless wavenumber, it has approximately the same behavior.

Fig. 2 shows the influence of various volume fraction on the phase velocity for double bonded micro sandwich cylindrical shells with porous core and CNTRC face sheets. It

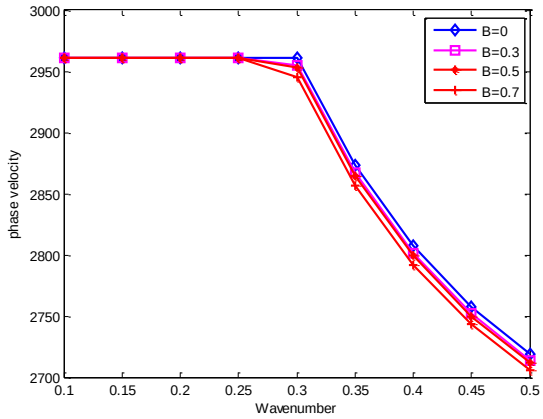

Fig. 4 The influence of Skempton coefficient on the phase velocity for double-bonded micro sandwich cylindrical shell

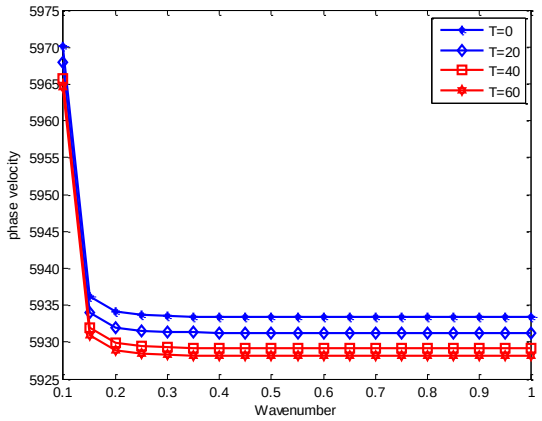

Fig. 5 The influence of temperature change on the phase velocity

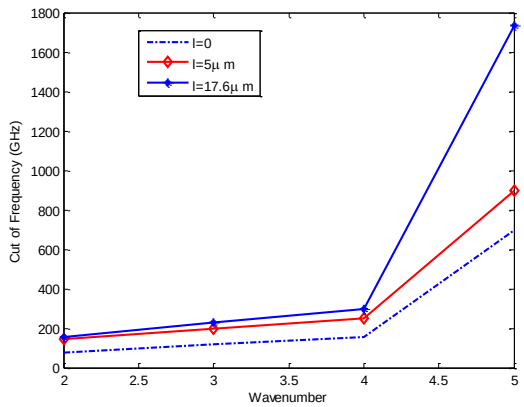

Fig. 6 The influence of the material length scale parameter on the cut of frequency

can be seen that by increasing of the CNT volume fraction, the phase velocity increases.

Fig. 3 presents the influence of the porosity coefficient on the phase velocity. It is shown that by increasing of this coefficient, the phase velocity enhances for lower wave number and vice versa for higher wave number. The free space volume of the micro sandwich cylindrical shell increases as the porosity coefficient increases, and the weight of the structure decreases, as well as its stiffness.

But the effect of the structure's stiffness is higher, so the phase velocity of double-bonded micro sandwich cylindrical shell increases for lower wave number with an increase in the porosity coefficient.

Fig. 4 investigates the influence of Skempton coefficient on the phase velocity for double-bonded micro sandwich cylindrical shell. It can be seen that by increasing of Skempton coefficient, the phase velocity decreases for higher wave number and the results become approximately the constant.

The influence of temperature change on the phase velocity is shown in Fig. 5. It is depicted that with increasing of the temperature change, the phase velocity decreases.

Fig. 6 shows the influence of the material length scale parameter on the cut of frequency for double-bonded micro sandwich cylindrical shell. It can be seen that by increasing of the material length scale parameter, the cut of frequency increases, because the stiffness of micro structure increases.

7. Conclusions

In this paper, wave propagation of double-bonded Cooper-Naghdi micro sandwich cylindrical shells with porous core and carbon nanotube reinforced composite (CNTRC) face sheets are investigated subjected to multi-physical loadings with temperature dependent material properties. The governing equations of motion are derived by Hamilton's principle. The following results are obtained from this research:

1. With increasing n in lower dimensionless wavenumber, the difference between curves for phase velocity increases; while for higher dimensionless wavenumber, it has approximately the same behavior.
2. It is shown that by increasing of the CNT volume fraction, the phase velocity increases and vice versa for temperature change.
3. It can be seen that by increasing of Skempton coefficient, the phase velocity decreases for higher wave number and the results become approximately the constant.
4. It is seen that by increasing of the material length scale parameter, the cut of frequency increases, because the stiffness of micro structure increases.
5. It is considered that by increasing of porosity coefficient, the phase velocity enhances for lower wave number and vice versa for higher wave number. The free space volume of the micro sandwich cylindrical shell increases as the porosity coefficient increases, and the weight of the structure decreases, as well as its stiffness. But the effect of the structure's stiffness is higher, so the phase velocity of double-bonded micro sandwich cylindrical shell increases for lower wave number with an increase in the porosity coefficient.

Acknowledgment

The authors would like to thank the reviewers for their valuable comments and suggestions to improve the clarity of this work and grateful to the Iranian Nanotechnology Development Committee for their financial support and the University of Kashan for supporting this work by Grant No. 891238/3.

References

Al-Kamal, M.K. (2019), "Nominal axial and flexural strengths of high-strength concrete columns", *Comput. Concrete*, **24**(1), 85-94. https://doi.org/10.12989/cac.2019.24.1.085.

Ansari, R., Gholami, R. and Sahmani, S. (2011), "Free vibration analysis of size-dependent functionally graded microbeams based on the strain gradient Timoshenko beam theory", *Compos. Struct.*, **94**, 221-228. https://doi.org/10.1016/j.compstruct.2011.06.024.

Arani, A.G., Pourjamshidian, M. and Arefi, M. (2017), "Influence of electro-magneto-thermal environment on the wave propagation analysis of sandwich nano-beam based on nonlocal strain gradient theory and shear deformation theories", *Smart Struct. Syst.*, **20**(3), 329-342. https://doi.org/10.12989/sss.2017.20.3.329.

Cong, P.H., Chienc, T.M., Khoa, N.D. and Duc, N.D. (2018), "Nonlinear thermo mechanical buckling and post-buckling response of porous FGM plates using Reddy's HSDT", *Aerosp. Sci. Technol.*, **77**, 419-428. https://doi.org/10.1016/j.ast.2018.03.020.

Do, T.V., Nguyen, D.K., Duc, N.D., Doan, D.H. and Bui, T.Q. (2017), "Analysis of bi-directional functionally graded plates by FEM and a new third-order shear deformation plate theory", *Thin Wall. Struct.*, **119**, 687-699. https://doi.org/10.1016/j.tws.2017.07.022.

Doyle, J.F. (1997), *Wave Propagation in Structures*, New York, USA.

Duc, N.D. (2013), "Nonlinear dynamic response of imperfect eccentrically stiffened FGM double curved shallow shells on elastic foundation", *Compos. Struct.*, **99**, 88-96. https://doi.org/10.1016/j.compstruct.2012.11.017.

Duc, N.D. (2016), "Nonlinear thermo-electro-mechanical dynamic response of shear deformable piezoelectric sigmoid functionally graded sandwich circular cylindrical shells on elastic foundations", *J. Sandw. Struct. Mater.*, 1-28. https://doi.org/10.1177/1099636216653266.

Duc, N.D. and Cong, P.H. (2018), "Nonlinear dynamic response and vibration of sandwich composite plates with negative Poisson's ratio in auxetic honeycombs", *J. Sandw. Struct. Mater.*, **20**(6), 692-717. https://doi.org/10.1177/1099636216674729.

Duc, N.D., Cong, P.H., Anh, V.M., Quang, V.D., Tran, P., Tuan, N.D. and Thinh, N.H. (2015), "Mechanical and thermal stability of eccentrically stiffened functionally graded conical shell panels resting on elastic foundations and in thermal environment", *Compos/ Struct.*, **132**, 597-609. https://doi.org/10.1016/j.compstruct.2015.05.072.

Duc, N.D., Hadavinia, H., Quan, T.Q. and Khoa, N.D. (2019), "Free vibration and nonlinear dynamic response of imperfect nanocomposite FGCNTRC double curved shallow shells in thermal environment", *Eur. J. Mech., A Solid.*, **75**, 355-366. https://doi.org/10.1016/j.euromechsol.2019.01.024.

Erofeev, V.I. and Mal'khanov, A.O. (2017), "Localized strain waves in a nonlinearly elastic conducting medium interacting with a magnetic field", *Mech. Solid.*, **52**(2), 224-231. https://doi.org/10.3103/S0025654417020121.

Farahani, H. and Barati, F. (2015), "Vibration of sumberged functionally graded cylindrical shell based on first order shear deformation theory using wave propagation method", *Struct.*

Eng. Mech., **53**(3), 575-587. https://doi.org/10.12989/sem.2015.53.3.575.

Farajpour, A., Hairi Yazdi, MR., Rastgoo, A., Loghmani, M. and Mohammadi, M. (2016), "Nonlocal nonlinear plate model for large amplitude vibration of magneto-electro-elastic nanoplate", *Compos. Struct.*, **140**, 323-336. https://doi.org/10.1016/j.compstruct.2015.12.039.

Frikha, A., Zghal, S. and Dammak, F. (2018), "Dynamic analysis of functionally graded carbon nanotubes-reinforced plate and shell structures using a double directors finite shell element", *Aerosp. Sci. Technol.*, **78**, 438-451. https://doi.org/10.1016/j.ast.2018.04.048.

Ghorbanpour Arani, A., Jalilvand, A. and Haghparast, E. (2018), "Theoretical investigation on wave propagation in embedded DWBNNT conveying ferrofluid via stress and strain-inertia gradient elasticity", *Proc. Inst. Mech. Eng., Part L: J. Mater.: Des. Appl.*, **232**(9), 719-732. https://doi.org/10.1177/1464420716644761.

Ghorbanpour Arani, A., Jamali, M., Mosayyebi, M. and Kolahchi, R. (2016), "Wave propagation in FG-CNT-reinforced piezoelectric composite micro plates using viscoelastic quasi-3D sinusoidal shear deformation theory", *Compos. Part B: Eng.*, **95**, 209-224. https://doi.org/10.1016/j.compositesb.2016.03.077.

Ghorbanpour Arani, A., Khani Arani, H. and Khoddami Maraghi, Z. (2016), "Vibration analysis of sandwich composite micro-plate under electro-magneto-mechanical loadings", *Appl. Math. Model.*, **40**, 10596-10615. https://doi.org/10.1016/j.apm.2016.07.033.

Ghorbanpour Arani, A., Rousta Navi, B. and Mohammadimehr, M. (2016), "Surface stress and agglomeration effects on nonlocal biaxial buckling polymeric nanocomposite plate reinforced by CNT using various approaches", *Adv. Composite Mater.*, **25**(5), 423-441. https://doi.org/10.1080/09243046.2015.1052189.

Ghorbanpour Arani, A.H., Rastgoo, A., Hafizi Bidgoli, A., Kolahchi, R. and Ghorbanpour Arani, A. (2017), "Wave propagation of coupled double-DWBNNTs conveying fluid-systems using different nonlocal surface piezoelasticity theories", *Mech. Adv. Mater. Struct.*, **24**(14), 1159-1179. https://doi.org/10.1080/15376494.2016.1227488.

Hossein Hosseini, S.M., Duczek, S. and Gabbert, U. (2013), "Non-reflecting boundary condition for Lamb wave propagation problems in honeycomb and CFRP plates using dashpot elements", *Compos. Part B: Eng.*, **54**, 1-10. https://doi.org/10.1016/j.compositesb.2013.04.061.

Hossein Hosseini, S.M., Kharaghani, A., Kirsch, C. and Gabbert, U. (2013), "Numerical simulation of Lamb wave propagation in metallic foam sandwich structures: a parametric study", *Compos. Struct.*, **97**, 387-400. https://doi.org/10.1016/j.compstruct.2012.10.039.

Jamali, M., Arani, A.G., Mosayyebi, M., Kolahchi, R. and Esfahani, R.T. (2017), "Wave propagation behavior of coupled viscoelastic FG-CNTRPC micro plates subjected to electro-magnetic fields surrounded by orthotropic visco-Pasternak foundation", *Microsyst. Technol.*, **23**(8), 3791-3816. https://doi.org/10.1007/s00542-016-3232-5.

Kakar, R. (2015), "SH-wave propagation in a heterogeneous layer over an inhomogeneous isotropic elastic half-space", *Earthq. Struct.*, **9**(2), 305-320. https://doi.org/10.12989/eas.2015.9.2.305.

Ke, L.L., Liu, C.H. and Wang, Y. (2015), "Free vibration of nonlocal piezoelectric nanoplates under various boundary conditions", *Physica E*, **66**, 93-106. https://doi.org/10.1016/j.physe.2014.10.002.

Khoa, N.D., Thiem, H.T. and Duc, N.D. (2019), "Nonlinear buckling and postbuckling of imperfect piezoelectric S-FGM circular cylindrical shells with metal-ceramic-metal layers in thermal environment using Reddy's third-order shear deformation shell theory", *Mech. Adv. Mater. Struct.*, **26**(3), 248-259. https://doi.org/10.1080/15376494.2017.1341583.

Li, Y.S. and Pan, E. (2015), "Static bending and free vibration of a functionally graded piezoelectric microplate based on the modified couple-stress theory", *Int. J. Eng. Sci.*, **97**, 40-59. https://doi.org/10.1016/j.ijengsci.2015.08.009.

Mohammadimehr, M. and Alimirzaei, S. (2016), "Nonlinear static and vibration analysis of Euler-Bernoulli composite beam model reinforced by FG-SWCNT with initial geometrical imperfection using FEM", *Struct. Eng. Mech.*, **59**(3), 431-454. http://dx.doi.org/10.12989/sem.2016.59.3.431.

Mohammadimehr, M. and Mostafavifar, M. (2016), "Free vibration analysis of sandwich plate with a transversely flexible core and FG-CNTs reinforced nanocomposite face sheets subjected to magnetic field and temperature-dependent material properties using SGT", *Compos. Part B*, **94**, 253-270. https://doi.org/10.1016/j.compositesb.2016.03.030.

Mohammadimehr, M. and Shahedi, S. (2016), "High-order buckling and free vibration analysis of two types sandwich beam including AL or PVC-foam flexible core and CNTs reinforced nanocomposite face sheets using GDQM", *Compos. Part B*, **108**, 91-107. https://doi.org/10.1016/j.compositesb.2016.09.040.

Mohammadimehr, M., Farahi, M.J. and Alimirzaei, S. (2016a), "Vibration and wave propagation analysis of twisted micro-beam using strain gradient theory", *Appl. Math. Mech. (English Ed.)*, **37**(10), 1375-1392. https://doi.org/10.1007/s10483-016-2138-9.

Mohammadimehr, M., Mohammadimehr, M.A. and Dashti, P. (2016c), "Size-dependent effect on biaxial and shear nonlinear buckling analysis of nonlocal isotropic and orthotropic micro-plate based on surface stress and modified couple stress theories using differential quadrature method", *Appl. Math. Mech. (English Ed.)*, **37**(4), 529-554. https://doi.org/10.1007/s10483-016-2045-9.

Mohammadimehr, M., Navi, B.R. and Arani, A.G. (2017b), "Dynamic stability of modified strain gradient theory sinusoidal viscoelastic piezoelectric polymeric functionally graded single-walled carbon nanotubes reinforced nanocomposite plate considering surface stress and agglomeration effects under hydro-thermo-electro-magneto-mechanical loadings", *Mech. Adv. Mater. Struct.*, **24**(16), 1325-1342. https://doi.org/10.1080/15376494.2016.1227507.

Mohammadimehr, M., Okhravi, S.V. and Akhavan Alavi, S.M. (2018), "Free vibration analysis of magneto-electro-elastic cylindrical composite panel reinforced by various distributions of CNTs with considering open and closed circuits boundary conditions based on FSDT", *J. Vib. Control*, **24**(8), 1551-1569. https://doi.org/10.1177/1077546316664022.

Mohammadimehr, M., Salemi, M. and Rousta Navi, B. (2016b), "Bending buckling and free vibration analysis of MSGT microcomposite Reddy plate reinforced by FG-SWCNTs with temprature-dependent material properties under hydro-thermo-mechanical loadings using DQM", *Compos. Struct.*, **138**, 361-380. https://doi.org/10.1016/j.compstruct.2015.11.055.

Mohammadimehr, M., Shahedi, S. and Rousta Navi, B. (2017a), "Nonlinear vibration analysis of FG-CNTRC sandwich Timoshenko beam based on modified couple stress theory subjected to longitudinal magnetic field using generalized differential quadrature method", *Proc. Inst. Mech. Eng., Part C: J. Mech. Eng. Sci.*, **231**(20), 3866-3885. https://doi.org/10.1177/0954406216653622.

Mohammadimehr, M., Zarei, H.B., Parakandeh, A. and Arani, A.G. (2017c), "Vibration analysis of double-bonded sandwich microplates with nanocomposite facesheets reinforced by symmetric and un-symmetric distributions of nanotubes under

multi physical fields", *Struct. Eng. Mech.*, **64**(3), 361-379. https://doi.org/10.12989/sem.2017.64.3.361.

Murmu, T., McCarthy, MA. and Adhikari, S. (2012), "Vibration response of double-walled carbon nanotubes subjected to an externally applied longitudinal magnetic field: A nanlocal elasticity approach", *J. Sound Vib.*, **331**, 5069-5086. https://doi.org/10.1016/j.jsv.2012.06.005.

Narendar, S. and Gopalakrishnan, S. (2012), "Study of terahertz wave propagation properties in nanoplates with surface and small-scale effects", *Int. J. Mech. Sci.*, **64**(1), 221-231. https://doi.org/10.1016/j.ijmecsci.2012.06.012.

Netrebko, A.V. (2013), "Wave propagation in an elastic structure modeling a split Hopkinson pressure bar", *Mech. Solid.*, **48**(4), 473-481. https://doi.org/10.3103/S0025654413040158.

Parate, K.N. and Kumar, R. (2019), "Shear strength model for reinforced concrete beam-column joints based on hybrid approach", *Comput. Concrete*, **23**(6), 377-398. https://doi.org/10.12989/cac.2019.23.6.377.

Porokhovs'kyi, V.V. (2009), "Plane problem of interaction between an elastic longitudinal wave and a cylindrical shell with axial cut", *J. Math. Sci.*, **160**(4), 443-452. https://doi.org/10.1007/s10958-009-9516-x.

Pourasghar, A. and Kamarian, S. (2016), "Thermoelastic response of CNT reinforced cylindrical panel resting on elastic foundation using theory of elasticity", *Mater. Des.*, **49**, 583-590. https://doi.org/10.1016/j.compositesb.2016.06.028.

Rajabi, J. and Mohammadimehr, M. (2019), "Bending analysis of a micro sandwich skew plate using extended Kantorovich method based on Eshelby-Mori-Tanaka approach", *Comput. Concrete*, **23**(5), 361-376. https://doi.org/10.12989/cac.2019.23.5.361.

Rasulova, N.B. and Shamilova, G.R. (2016), "Stress wave propagation in a rectangular bar", *Mech. Solid.*, **51**(4), 495-500. https://doi.org/10.1016/0020-7683(69)90020-1.

Rozhkova, E.V. (2018), "To the investigation of plane wave propagation in an elastic anisotropic media by a recursive operator method", *Mech. Solid.*, **53**(1), 33-44. https://doi.org/10.3103/S0025654418010041.

Safaei, B., Moradi-Dastjerdi, R., Qin, Z. and Chu, F. (2019), "Frequency-dependent forced vibration analysis of nanocomposite sandwich plate under thermo-mechanical loads", *Compos. Part B: Eng.*, **161**, 44-54. https://doi.org/10.1016/j.compositesb.2018.10.049.

Saidi, A.R., Bahaadini, R. and Majidi-Mozafari, K. (2019), "On vibration and stability analysis of porous plates reinforced by graphene platelets under aerodynamical loading", *Compos. Part B: Eng.*, **164**, 778-799. https://doi.org/10.1016/j.compositesb.2019.01.074.

Sellappan, P., Wang, E., Espinoza Santos, C.J., On, T. and Kriven, W.M. (2015), "Wave propagation through alumina-porous alumina laminates", *J. Eur. Ceram. Soc.*, **35**(1), 197-210. https://doi.org/10.1016/j.jeurceramsoc.2014.08.013.

Shamaev, A.S. and Shumilova, V.V. (2017), "Plane acoustic wave propagation through a composite of elastic and Kelvin-Voigt viscoelastic material layers", *Mech. Solid.*, **52**(1), 25-34. https://doi.org/10.3103/S0025654417010046.

Shariyat, M., Jahanshahi, S. and Rahimi, H. (2019) "Nonlinear Hermitian generalized hygrothermoelastic stress and wave propagation analyses of thick FGM spheres exhibiting temperature, moisture, and strain-rate material dependencies", *Compos. Struct.*, **229**, 111364. https://doi.org/10.1016/j.compstruct.2019.111364.

Sobhy, M. and Zenkour, A.M. (2018), "Magnetic field effect on thermomechanical buckling and vibration of viscoelastic sandwich nanobeams with CNT reinforced face sheets on a viscoelastic substrate", *Compos. Part B: Eng.*, **154**, 492-506. https://doi.org/10.1016/j.compositesb.2018.09.011.

Sorokin, S.V. and Grishina, S.V. (2004), "Analysis of wave propagation in sandwich beams with parametric stiffness modulations", *J. Sound Vib.*, **27** (3-5), 1063-1082. https://doi.org/10.1016/j.jsv.2003.03.005.

Tornabene, F. (2009), "Free vibration analysis of functionally graded conical, cylindrical shell and annular plate structures with a four-parameter power-law distribution", *Comput. Meth. Appl. Mech. Eng.*, **198**(37-40), 2911-2935. https://doi.org/10.1016/j.cma.2009.04.011.

Tornabene, F., Fantuzzi, N., Viola, E. and Batra, R.C. (2015), "Stress and strain recovery for functionally graded free-form and doubly-curved sandwich shells using higher-order equivalent single layer theory", *Compos. Struct.*, **119**(1), 67-89. https://doi.org/10.1016/j.compstruct.2014.08.005.

Tornabene, F., Liverani, L. and Caligiana, G. (2011), "FGM and laminated doubly curved shells and panels of revolution with a free-form meridian: A 2-D GDQ solution for free vibrations", *Int. J. Mech. Sci.*, **53**(6), 446-470. https://doi.org/10.1016/j.ijmecsci.2011.03.007.

Wu, K., Zhai, J., Xue, J., Xu, F. and Zhao, H. (2019), "Experimental study on shear damage and lateral stiffness of transfer column in SRC-RC hybrid structure", *Comput. Concrete*, **23**(5), 335-349. https://doi.org/10.12989/cac.2019.23.5.335.

Xu, X. and Deng, Z. (2016), "Wave propagation characteristics in thick conventional and auxetic cellular plates", *Acta Mechanica Solida Sinica*, **29**(2), 159-166. https://doi.org/10.1016/S0894-9166(16)30104-5.

Zghal, S., Frikha, A. and Dammak, F. (2018), "Mechanical buckling analysis of functionally graded power-based and carbon nanotubes-reinforced composite plates and curved panels", *Compos. Part B*, **150**, 165-183. https://doi.org/10.1016/j.compositesb.2018.05.037.

CC

Appendix A

Strain-displacement relations for each of face sheet and core can be expressed as follows

$$\begin{aligned}
\varepsilon_{xx} &= \frac{\partial U_x}{\partial x} = \frac{\partial u}{\partial x} + z\,\frac{\partial \beta_x}{\partial x} \\
\varepsilon_{\theta\theta} &= \frac{U_z}{R} + \frac{1}{R}\frac{\partial U_\theta}{\partial \theta} = \frac{1}{R}(w + \frac{\partial v}{\partial \theta} + z\,\frac{\partial \beta_\theta}{\partial \theta}) \\
\varepsilon_{z\theta} &= \frac{1}{2}(\frac{1}{R}\frac{\partial U_z}{\partial \theta} + \frac{\partial U_\theta}{\partial z} - \frac{v}{R}) = \frac{1}{2}(\frac{1}{R}\frac{\partial w}{\partial \theta} + \beta_\theta - \frac{v}{R}) \\
\varepsilon_{xz} &= \frac{1}{2}(\frac{\partial U_z}{\partial x} + \frac{\partial U_x}{\partial z}) = \frac{1}{2}(\frac{\partial w}{\partial x} + \beta_x) \\
\varepsilon_{\theta x} &= \frac{1}{2}(\frac{1}{R}\frac{\partial U_x}{\partial \theta} + \frac{\partial U_\theta}{\partial x}) = \frac{1}{2}(\frac{1}{R}(\frac{\partial u}{\partial \theta} + z\,\frac{\partial \beta_x}{\partial \theta}) + \frac{\partial v}{\partial x} + z\,\frac{\partial \beta_\theta}{\partial x}
\end{aligned} \tag{A1}$$

Appendix B

The various porous distribution types along thickness can be written as follows for core

$$\begin{aligned}
G(z) &= G_0(1 - e_1\cos((\frac{\pi}{2h})(z + \frac{h}{2}))) \\
E(z) &= E_0(1 - e_1\cos((\frac{\pi}{2h})(z + \frac{h}{2}))) \\
\rho(z) &= \rho_0(1 - e_1\cos((\frac{\pi}{2h})(z + \frac{h}{2})))
\end{aligned}$$

$$\begin{aligned}
G(z) &= G_0(1 - e_1\cos(\frac{\pi z}{h})) \\
E(z) &= E_0(1 - e_1\cos(\frac{\pi z}{h})) \\
\rho(z) &= \rho_0(1 - e_1\cos(\frac{\pi z}{h}))
\end{aligned} \tag{B1}$$

$$\begin{aligned}
G(z) &= G_0(1 - e_1) \\
E(z) &= E_0(1 - e_1) \\
\rho(z) &= \rho_0(1 - e_1)
\end{aligned}$$

where the initial shear modulus, Poisson's ratio and density are G_0=24 GPa, ν_0=0.3 and ρ_0=2700 kg/m^3.

The extended mixture approach is used for effective material properties of face sheets as follows

$$\begin{aligned}
E_{11} &= \eta_1 V_{NT} E_{11}^{NT} + V_m E_m \\
\frac{\eta_2}{E_{22}} &= \frac{V_{NT}}{E_{22}^{NT}} + \frac{V_m}{E_m} \\
\frac{\eta_3}{G_{12}} &= \frac{V_{NT}}{G_{12}^{NT}} + \frac{V_m}{G_m}
\end{aligned} \tag{B2}$$

where, η_i (i=1,2,3) are efficiency coefficients of nanotubes (NTs) including CNT and BNNT. These coefficients are listed in Table 1. E_{11}, E_{22} and G_{12} are the Young's modulii and the shear modulus of the NT, and V_{NT} and V_m are the volume fraction of the NT and the matrix, respectively. The material properties of SWCNTs and SWBNNTs for different temperatures are listed in Tables 2 and 3, respectively. Various distributions of NT are defined as

$$V_{NT}(z) = \begin{cases} V_{NT}^* & (UD - NT) \\ (1 + \frac{2z}{h})V_{NT}^* & (FG - V - NT) \\ 2(1 - \frac{|2z|}{h})V_{NT}^* & (FG - O - NT) \\ 2\frac{|2z|}{h}V_{NT}^* & (FG - X - NT) \end{cases} \tag{B3}$$

where

$$V_{NT}^* = \frac{w_{NT}}{w_{NT} + \left(\frac{\rho_{NT}}{\rho_m}\right)(1 - w_{NT})} \tag{B4}$$

where, w_{SWCNT} is the mass fraction of the nanotubes. ρ_{NT} and ρ_m are densities of NTs and the matrix, respectively.

Appendix C

δu_1:

$$\begin{aligned}
&-(D_{1,0} + A_{20})\frac{\partial^2 u_1}{\partial x^2} + \frac{D_{5,0}l^2}{4R^2}\frac{\partial^4 u_1}{\partial x^2 \partial \theta^2} - \frac{D_{5,0}l^2}{R^4}\frac{\partial^2 u_1}{\partial \theta^2} \\
&-\frac{1}{R^2}(D_{5,0} + C_{20})\frac{\partial^2 u_1}{\partial \theta^2} + \frac{D_{5,0}l^2}{4R^4}\frac{\partial^4 u_1}{\partial \theta^4} - \frac{D_{5,0}l^2}{4R}\frac{\partial^4 v_1}{\partial x^3 \partial \theta} \\
&+\frac{1}{R}(\frac{D_{5,0}l^2}{4R^2})\frac{\partial^2 v_1}{\partial x \partial \theta} - \frac{1}{R}(D_{3,0} + D_{5,0} + B_{20} + C_{20})\frac{\partial^2 v_1}{\partial x \partial \theta} \\
&-\frac{D_{5,0}l^2}{4R^3}\frac{\partial^4 v_1}{\partial x \partial \theta^3} - \frac{1}{R}(D_{3,0} + B_{20})\frac{\partial w_1}{\partial x} - \frac{D_{5,0}l^2}{2R^3}\frac{\partial^3 w_1}{\partial x \partial \theta^2} \\
&-\frac{1}{R}(\frac{D_{5,0}l^2}{4R} - \frac{D_{5,1}l^2}{2R^2})\frac{\partial^2 \beta_{\theta 1}}{\partial x \partial \theta} - \frac{1}{R}(D_{3,1} + D_{5,1} + B_{21} + C_{21})\frac{\partial^2 \beta_{\theta 1}}{\partial x \partial \theta} \\
&+\frac{1}{R^2}(\frac{5D_{5,0}l^2}{4R})\frac{\partial^2 \beta_{x1}}{\partial \theta^2} - \frac{1}{R^2}(C_{21} + D_{5,1})\frac{\partial^2 \beta_{x1}}{\partial \theta^2} - (D_{1,1} + A_{21})\frac{\partial^2 \beta_{x1}}{\partial x^2} \\
&-\frac{D_{5,1}l^2}{4R^3}\frac{\partial^4 \beta_{\theta 1}}{\partial x \partial \theta^3} + \frac{D_{5,1}l^2}{4R^4}\frac{\partial^4 \beta_{x1}}{\partial \theta^4} - \frac{D_{5,1}l^2}{4R}\frac{\partial^4 \beta_{\theta 1}}{\partial x^3 \partial \theta} + \frac{D_{5,1}l^2}{4R^2}\frac{\partial^4 \beta_{x1}}{\partial x^2 \partial \theta^2} \\
&+\frac{\partial}{\partial x}(\alpha_{11}\Delta T + \beta_{11}\Delta H)D_{1,0} + \frac{\partial}{\partial x}(\alpha_{22}\Delta T + \beta_{22}\Delta H)D_{3,0} \\
&-\frac{\partial N_{1,\varphi_0}}{\partial x} - \frac{\partial N_{1,\psi_0}}{\partial x} - N_{1,\varphi}\frac{\partial \varphi_1}{\partial x} - N_{1,\psi}\frac{\partial \psi_1}{\partial x} + I^{(1)}\frac{\partial^2 \beta_{x1}}{\partial t^2} + I^{(0)}\frac{\partial^2 u_1}{\partial t^2} = 0
\end{aligned} \tag{C1}$$

δv_1:

$$\begin{aligned}
&\frac{D_{5,0}l^2}{4}\frac{\partial^4 v_1}{\partial x^4} - D_{5,0}(\frac{l^2}{2R^2})\frac{\partial^2 v_1}{\partial x^2} - (D_{5,0} - C_{20})\frac{\partial^2 v_1}{\partial x^2} - \frac{1}{R^2}(\frac{D_{5,0}l^2}{4R^2})\frac{\partial^2 v_1}{\partial \theta^2} \\
&-\frac{1}{R^2}(D_{2,0} + A_{20})\frac{\partial^2 v_1}{\partial \theta^2} + \frac{D_{5,0}l^2}{4R^2}\frac{\partial^4 v_1}{\partial x^2 \partial \theta^2} + \frac{1}{R^2}(\frac{D_{5,0}l^2}{4R^2} + D_{4,0}k_s)v_1 \\
&-\frac{D_{5,0}l^2}{4R}\frac{\partial^4 u_1}{\partial x^3 \partial \theta} - \frac{D_{5,0}l^2}{4R^3}\frac{\partial^4 u_1}{\partial x \partial \theta^3} + \frac{1}{R}(\frac{D_{5,0}l^2}{4R^2} - D_{3,0} - D_{5,0})\frac{\partial^2 u_1}{\partial x \partial \theta} \\
&+\frac{3D_{5,0}l^2}{4R^2}\frac{\partial^3 w_1}{\partial x^2 \partial \theta} + \frac{D_{5,0}l^2}{4R^4}\frac{\partial^3 w_1}{\partial \theta^3} - \frac{1}{R^2}(D_{2,0} + \frac{D_{5,0}l^2}{4R^2} + D_{4,0}k_s)\frac{\partial w_1}{\partial \theta} \\
&-\frac{1}{R}(\frac{D_{5,0}l^2}{2R} + D_{5,1} + D_{3,1} + \frac{D_{5,1}l^2}{4R^2})\frac{\partial^2 \beta_{x1}}{\partial x \partial \theta} - \frac{1}{R^2}(\frac{D_{5,0}l^2}{4R} + D_{2,1})\frac{\partial^2 \beta_{\theta 1}}{\partial \theta^2} \\
&-(\frac{3D_{5,0}l^2}{4R} + D_{5,1} + \frac{D_{5,1}l^2}{4R^2})\frac{\partial^2 \beta_{\theta 1}}{\partial x^2} + \frac{D_{5,1}l^2}{4R^2}\frac{\partial^4 \beta_{\theta 1}}{\partial x^2 \partial \theta^2} - \frac{D_{5,1}l^2}{4R^3}\frac{\partial^4 \beta_{x1}}{\partial x \partial \theta^3} \\
&+\frac{D_{5,1}l^2}{4}\frac{\partial^4 \beta_{\theta 1}}{\partial x^4} - \frac{1}{R}(\frac{D_{5,0}l^2}{4R^2} + D_{4,0}k_s)\beta_{\theta 1} - \frac{D_{5,1}l^2}{4R}\frac{\partial^4 \beta_{x1}}{\partial x^3 \partial \theta} \\
&-\frac{1}{R}(\frac{\partial N_{2,\varphi_0}}{\partial \theta} + \frac{\partial N_{2,\psi_0}}{\partial \theta}) - \frac{1}{R}(N_{2,\varphi}\frac{\partial \varphi_1}{\partial \theta} + N_{2,\psi}\frac{\partial \psi_1}{\partial \theta}) \\
&-\frac{1}{R}(-N_{4,\varphi}\frac{\partial \varphi_1}{\partial \theta} - N_{4,\psi}\frac{\partial \psi_1}{\partial \theta}) + I^{(1)}\frac{\partial^2 \beta_{\theta 1}}{\partial t^2} + I^{(0)}\frac{\partial^2 v_1}{\partial t^2} = 0
\end{aligned} \tag{C2}$$

δw_1 :

$$
\begin{aligned}
&\frac{D_{5,0}l^2}{4}\frac{\partial^4 w_1}{\partial x^4}-D_{5,0}\left(\frac{l^2}{4R^2}+k_s\right)\frac{\partial^2 w_1}{\partial x^2}+\frac{D_{5,0}l^2}{2R^2}\frac{\partial^4 w_1}{\partial x^2\partial\theta^2}+\frac{D_{5,0}l^2}{4R^4}\frac{\partial^4 w_1}{\partial\theta^4}\\
&-\frac{1}{R^2}\left(\frac{D_{5,0}l^2}{4R^2}+D_{4,0}k_s\right)\frac{\partial^2 w_1}{\partial\theta^2}+\frac{D_{2,0}}{R^2}w_1+\frac{D_{3,0}}{R}\frac{\partial u_1}{\partial x}+\frac{D_{5,0}l^2}{2R^3}\frac{\partial^3 u_1}{\partial x\,\partial\theta^2}\\
&-\frac{3D_{5,0}l^2}{4R^2}\frac{\partial^3 v_1}{\partial x^2\partial\theta}+\frac{1}{R^2}\left(D_{2,0}+\frac{D_{5,0}l^2}{4R^2}+D_{4,0}k_s\right)\frac{\partial v_1}{\partial\theta}-\frac{D_{5,0}l^2}{4R^4}\frac{\partial^3 v_1}{\partial\theta^3}\\
&-\frac{D_{5,0}l^2}{4R^2}\frac{\partial^3\beta_{x1}}{\partial x\,\partial\theta^2}-\frac{D_{5,0}l^2}{4}\frac{\partial^3\beta_{x1}}{\partial x^3}+\left(\frac{D_{5,0}l^2}{4R^2}-D_{5,0}k_s+\frac{D_{3,1}}{R}\right)\frac{\partial\beta_{x1}}{\partial x}\\
&-\frac{D_{5,0}l^2}{4R^3}\frac{\partial^3\beta_{\theta1}}{\partial\theta^3}-\frac{1}{R}\left(\frac{D_{5,0}l^2}{4R^2}+D_{4,0}k_s-\frac{D_{2,1}}{R}\right)\frac{\partial\beta_{\theta1}}{\partial\theta}\\
&-\frac{1}{2R}\left(\frac{D_{5,0}l^2}{2}+\frac{D_{5,1}l^2}{R}\right)\frac{\partial^3\beta_{\theta1}}{\partial x^2\partial\theta}-\frac{1}{R}((\alpha_{11}\Delta T+\beta_{11}\Delta H)D_{3,0})\\
&-\frac{1}{R^2}(\alpha_{22}\Delta T+\beta_{22}\Delta H)D_{2,0})-\frac{1}{R}(-N_{2,\varphi_0}-N_{2,\varphi}\varphi_1-N_{2,\psi_0}-N_{2,\psi}\psi_1)\\
&+\frac{1}{R}N_{4,\varphi}\frac{\partial^2\varphi_1}{\partial\theta^2}+\frac{1}{R}N_{4,\psi}\frac{\partial^2\psi_1}{\partial\theta^2}+N_{5,\varphi}\frac{\partial^2\varphi_1}{\partial x^2}+N_{5,\psi}\frac{\partial^2\psi_1}{\partial x^2}+I^{(0)}\frac{\partial^2 w_1}{\partial t^2}\\
&-q(x,\theta)+k_{w1}w_1-k_{w2}(w_2-w_1)-k_{G1}\nabla^2 w_1+k_{G2}\nabla^2(w_2-w_1)=0
\end{aligned}
\tag{C3}
$$

$\delta\beta_{x1}$:

$$
\begin{aligned}
&-\left(\frac{D_{5,0}l^2}{4}\right)\frac{\partial^2\beta_{x1}}{\partial x^2}-(D_{1,2}+A_{22})\frac{\partial^2\beta_{x1}}{\partial x^2}+\frac{D_{5,2}l^2}{4R^2}\frac{\partial^4\beta_{x1}}{\partial x^2\partial\theta^2}+\frac{D_{5,2}l^2}{4R^4}\frac{\partial^4\beta_{x1}}{\partial\theta^4}\\
&-\frac{1}{R^2}\left(D_{5,0}l^2-\frac{D_{5,1}l^2}{2R}\right)\frac{\partial^2\beta_{x1}}{\partial\theta^2}-\frac{1}{R^2}(D_{5,2}+C_{22})\frac{\partial^2\beta_{x1}}{\partial\theta^2}+\left(\frac{D_{5,0}l^2}{4R^2}\right)\beta_{x1}\\
&+(D_{5,0}k_s+C_{20})\beta_{x1}-\frac{1}{R}\left(-\frac{3D_{5,0}l^2}{4}+\frac{D_{5,1}l^2}{2R}\right)\frac{\partial^2\beta_{\theta1}}{\partial x\,\partial\theta}\\
&-\frac{1}{R}(D_{3,2}+D_{5,2}+C_{22}+B_{22})\frac{\partial^2\beta_{\theta1}}{\partial x\,\partial\theta}-\frac{D_{5,2}l^2}{4R^3}\frac{\partial^4\beta_{\theta1}}{\partial x\,\partial\theta^3}-\frac{D_{5,2}l^2}{4R}\frac{\partial^4\beta_{\theta1}}{\partial x^3\partial\theta}\\
&+\frac{1}{R^2}\left(\frac{5D_{5,0}l^2}{4R}\right)\frac{\partial^2 u_1}{\partial\theta^2}-\frac{1}{R^2}(D_{5,1}+C_{21})\frac{\partial^2 u_1}{\partial\theta^2}-\frac{1}{R}\left(\frac{D_{5,0}l^2}{2R}+\frac{D_{5,1}l^2}{4R^2}\right)\frac{\partial^2 v_1}{\partial x\,\partial\theta}\\
&-\frac{1}{R}(+D_{3,1}+D_{5,1}+C_{21}+B_{21})\frac{\partial^2 v_1}{\partial x\,\partial\theta}+\frac{D_{5,0}l^2}{4}\frac{\partial^3 w_1}{\partial x^3}+\frac{D_{5,0}l^2}{4R^2}\frac{\partial^3 w_1}{\partial x\,\partial\theta^2}\\
&-\left(\frac{D_{5,0}l^2}{4R^2}\right)\frac{\partial w_1}{\partial x}-\left(-D_{5,0}k_s+\frac{D_{3,1}}{R}-C_{20}+\frac{1}{R}B_{21}\right)\frac{\partial w_1}{\partial x}-\frac{D_{5,1}l^2}{4R^3}\frac{\partial^4 v_1}{\partial x\,\partial\theta^3}\\
&-(D_{1,1}+A_{21})\frac{\partial^2 u_1}{\partial x^2}+\frac{D_{5,1}l^2}{4R^4}\frac{\partial^4 u_1}{\partial\theta^4}+\frac{D_{5,1}l^2}{4R^2}\frac{\partial^4 u_1}{\partial x^2\partial\theta^2}-\frac{D_{5,1}l^2}{4R}\frac{\partial^4 v_1}{\partial x^3\partial\theta}\\
&-\frac{\partial M_{1,\varphi_0}}{\partial x}-\frac{\partial M_{1,\psi_0}}{\partial x}-M_{1,\varphi}\frac{\partial\varphi_1}{\partial x}-M_{1,\psi}\frac{\partial\psi_1}{\partial x}-N_{5,\varphi}\frac{\partial\varphi_1}{\partial x}-N_{5,\psi}\frac{\partial\psi_1}{\partial x}\\
&+I^{(2)}\frac{\partial^2\beta_{x1}}{\partial t^2}+I^{(1)}\frac{\partial^2 u_1}{\partial t^2}=0
\end{aligned}
\tag{C4}
$$

$\delta\beta_{\theta1}$:

$$
\begin{aligned}
&\frac{D_{5,2}l^2}{4}\frac{\partial^4\beta_{\theta1}}{\partial x^4}-(D_{5,0}l^2+\frac{D_{5,2}l^2}{2R^2}+\frac{D_{5,1}l^2}{2R})\frac{\partial^2\beta_{\theta1}}{\partial x^2}-(D_{5,2}+C_{22})\frac{\partial^2\beta_{\theta1}}{\partial x^2}+\frac{D_{5,2}l^2}{4R^2}\frac{\partial^4\beta_{\theta1}}{\partial x^2\partial\theta^2}\\
&+\frac{D_{5,1}l^2}{4}\frac{\partial^4 v_1}{\partial x^4}-\frac{1}{R^2}\left(\frac{D_{5,0}l^2}{4}\right)\frac{\partial^2\beta_{\theta1}}{\partial\theta^2}-\frac{1}{R^2}(D_{2,2}+A_{22})\frac{\partial^2\beta_{\theta1}}{\partial\theta^2}-\frac{1}{R}\left(-\frac{3D_{5,0}l^2}{4}+\frac{D_{5,1}l^2}{2R}\right)\frac{\partial^2\beta_{x1}}{\partial x\,\partial\theta}\\
&-\frac{1}{R}(D_{3,2}+D_{5,2}+B_{22}+C_{22})\frac{\partial^2\beta_{x1}}{\partial x\,\partial\theta}-\frac{D_{5,1}l^2}{4R^3}\frac{\partial^4 u_1}{\partial x\,\partial\theta^3}-\frac{D_{5,2}l^2}{4R^3}\frac{\partial^4\beta_{x1}}{\partial x\,\partial\theta^3}-\frac{D_{5,2}l^2}{4R}\frac{\partial^4\beta_{x1}}{\partial x^3\partial\theta}\\
&-\frac{1}{R}\left(\frac{D_{5,0}l^2}{4R}-\frac{D_{5,1}l^2}{2R^2}\right)\frac{\partial^2 u_1}{\partial x\,\partial\theta}-\frac{1}{R}(+D_{3,1}+D_{5,1}+B_{21}+C_{21})\frac{\partial^2 u_1}{\partial x\,\partial\theta}-\left(\frac{3D_{5,0}l^2}{4R}+\frac{D_{5,1}l^2}{4R^2}\right)\frac{\partial^2 v_1}{\partial x^2}\\
&-(D_{5,1}+C_{21})\frac{\partial^2 v_1}{\partial x^2}-\frac{1}{R^2}\left(\frac{D_{5,0}l^2}{4R}\right)\frac{\partial^2 v_1}{\partial\theta^2}-\frac{1}{R^2}(D_{2,1}+A_{21})\frac{\partial^2 v_1}{\partial\theta^2}-\frac{1}{R}\left(\frac{D_{5,0}l^2}{4R^2}\right)v_1\\
&-\frac{1}{R}(C_{20}+k_sD_{4,0})v_1+\frac{1}{R}\left(\frac{D_{5,0}l^2}{4}+\frac{D_{5,1}l^2}{2R}\right)\frac{\partial^3 w_1}{\partial x^2\partial\theta}+\frac{D_{5,0}l^2}{4R^3}\frac{\partial^3 w_1}{\partial\theta^3}+\frac{1}{R}\left(\frac{D_{5,0}l^2}{4R^2}\right)\frac{\partial w_1}{\partial\theta}\\
&+\frac{1}{R}\left(+k_sD_{4,0}-\frac{D_{2,1}}{R}+C_{20}-\frac{A_{2,1}}{R}\right)\frac{\partial w_1}{\partial\theta}+\frac{D_{5,1}l^2}{4R^2}\frac{\partial^4 v_1}{\partial x^2\partial\theta^2}-\frac{D_{5,1}l^2}{4R}\frac{\partial^4 u_1}{\partial x^3\partial\theta}\\
&+\left(\frac{D_{5,0}l^2}{4R^2}\right)\beta_{\theta1}+(k_sD_{4,0}+C_{20})\beta_{\theta1}-\frac{1}{R}\left(\frac{\partial M_{2,\varphi_0}}{\partial\theta}+\frac{\partial M_{2,\psi_0}}{\partial\theta}\right)-\frac{1}{R}M_{2,\varphi}\frac{\partial\varphi_1}{\partial\theta}\\
&-\frac{1}{R}M_{2,\psi}\frac{\partial\psi_1}{\partial\theta}-N_{4,\varphi}\frac{\partial\varphi_1}{\partial\theta}-N_{4,\psi}\frac{\partial\psi_1}{\partial\theta}+I^{(1)}\frac{\partial^2 v_1}{\partial t^2}+I^{(2)}\frac{\partial^2\beta_{\theta1}}{\partial t^2}=0
\end{aligned}
\tag{C5}
$$

$\delta\varphi_1$:

$$
\begin{aligned}
&N_{5,\varphi}\left(\frac{\partial^2 w_1}{\partial x^2}+\frac{\partial \beta_{x1}}{\partial x}\right)+N_{1,D}\frac{\partial^2\varphi_1}{\partial x^2}+N_{1,B}\frac{\partial^2\psi_1}{\partial x^2}+N_{4,\varphi}\left(\frac{1}{R}\frac{\partial^2 w_1}{\partial\theta^2}+\frac{\partial\beta_{\theta1}}{\partial\theta}-\frac{1}{R}\frac{\partial v_1}{\partial\theta}\right)\\
&+N_{2,B}\frac{\partial^2\varphi_1}{\partial\theta^2}+N_{2,D}\frac{\partial^2\psi_1}{\partial\theta^2}+N_{1,\varphi}\frac{\partial u_1}{\partial x}+M_{1,\varphi}\frac{\partial\beta_{x1}}{\partial x}+\frac{1}{R}N_{2,\varphi}\left(w_1+\frac{\partial v_1}{\partial\theta}\right)+M_{2,\varphi}\frac{\partial\beta_{\theta1}}{\partial\theta}\\
&-N_{3,D1}\varphi_0-N_{3,D}\varphi_1-N_{3,B1}\varphi_0-N_{3,B}\varphi_1=0
\end{aligned}
\tag{C6}
$$

$\delta\psi_1$:

$$
\begin{aligned}
&N_{5,\psi}\left(\frac{\partial^2 w_1}{\partial x^2}+\frac{\partial \beta_{x1}}{\partial x}\right)+N_{1,B}\frac{\partial^2\varphi_1}{\partial x^2}+N_{1,B1}\frac{\partial^2\psi_1}{\partial x^2}+N_{4,\psi}\left(\frac{1}{R}\frac{\partial^2 w_1}{\partial\theta^2}+\frac{\partial\beta_{\theta1}}{\partial\theta}-\frac{1}{R}\frac{\partial v_1}{\partial\theta}\right)\\
&+N_{2,D}\frac{\partial^2\varphi_1}{\partial\theta^2}+N_{2,B1}\frac{\partial^2\psi_1}{\partial\theta^2}+N_{1,\psi}\frac{\partial u_1}{\partial x}+M_{1,\psi}\frac{\partial\beta_{x1}}{\partial x}+\frac{1}{R}N_{2,\psi}\left(w_1+\frac{\partial v_1}{\partial\theta}\right)+M_{2,\psi}\frac{\partial\beta_{\theta1}}{\partial\theta}\\
&-N_{3,B1}\varphi_0-N_{3,B}\varphi_1-N_{3,D2}\psi_0-N_{3,B2}\psi_1=0
\end{aligned}
\tag{C7}
$$

δu_2 :

$$
\begin{aligned}
&-(D_{1,0}+A_{20})\frac{\partial^2 u_2}{\partial x^2}+\frac{D_{5,0}l^2}{4R^2}\frac{\partial^4 u_2}{\partial x^2\partial\theta^2}-\frac{D_{5,0}l^2}{R^4}\frac{\partial^2 u_2}{\partial\theta^2}\\
&-\frac{1}{R^2}(D_{5,0}+C_{20})\frac{\partial^2 u_2}{\partial\theta^2}+\frac{D_{5,0}l^2}{4R^4}\frac{\partial^4 u_2}{\partial\theta^4}-\frac{D_{5,0}l^2}{4R}\frac{\partial^4 v_2}{\partial x^3\partial\theta}\\
&+\frac{1}{R}\left(\frac{D_{5,0}l^2}{4R^2}\right)\frac{\partial^2 v_2}{\partial x\,\partial\theta}-\frac{1}{R}(D_{3,0}+D_{5,0}+B_{20}+C_{20})\frac{\partial^2 v_2}{\partial x\,\partial\theta}\\
&-\frac{D_{5,0}l^2}{4R^3}\frac{\partial^4 v_2}{\partial x\,\partial\theta^3}-\frac{1}{R}(D_{3,0}+B_{20})\frac{\partial w_2}{\partial x}-\frac{D_{5,0}l^2}{2R^3}\frac{\partial^3 w_2}{\partial x\,\partial\theta^2}\\
&-\frac{1}{R}\left(\frac{D_{5,0}l^2}{4R}-\frac{D_{5,1}l^2}{2R^2}\right)\frac{\partial^2\beta_{\theta2}}{\partial x\,\partial\theta}-\frac{1}{R}(D_{3,1}+D_{5,1}+B_{21}+C_{21})\frac{\partial^2\beta_{\theta2}}{\partial x\,\partial\theta}\\
&+\frac{1}{R^2}\left(\frac{5D_{5,0}l^2}{4R}\right)\frac{\partial^2\beta_{x2}}{\partial\theta^2}-\frac{1}{R^2}(C_{21}+D_{5,1})\frac{\partial^2\beta_{x2}}{\partial\theta^2}-(D_{1,1}+A_{21})\frac{\partial^2\beta_{x2}}{\partial x^2}\\
&-\frac{D_{5,1}l^2}{4R^3}\frac{\partial^4\beta_{\theta2}}{\partial x\,\partial\theta^3}+\frac{D_{5,1}l^2}{4R^4}\frac{\partial^4\beta_{x2}}{\partial\theta^4}-\frac{D_{5,1}l^2}{4R}\frac{\partial^4\beta_{\theta2}}{\partial x^3\partial\theta}+\frac{D_{5,1}l^2}{4R^2}\frac{\partial^4\beta_{x2}}{\partial x^2\partial\theta^2}\\
&+\frac{\partial}{\partial x}(\alpha_{11}\Delta T+\beta_{11}\Delta H)D_{1,0}+\frac{\partial}{\partial x}(\alpha_{22}\Delta T+\beta_{22}\Delta H)D_{3,0}\\
&-\frac{\partial N_{1,\varphi_0}}{\partial x}-\frac{\partial N_{1,\psi_0}}{\partial x}-N_{1,\varphi}\frac{\partial\varphi_2}{\partial x}-N_{1,\psi}\frac{\partial\psi_2}{\partial x}+I^{(1)}\frac{\partial^2\beta_{x2}}{\partial t^2}+I^{(0)}\frac{\partial^2 u_2}{\partial t^2}=0
\end{aligned}
\tag{C8}
$$

δv_2 :

$$
\begin{aligned}
&\frac{D_{5,0}l^2}{4}\frac{\partial^4 v_2}{\partial x^4}-D_{5,0}\left(\frac{l^2}{2R^2}\right)\frac{\partial^2 v_2}{\partial x^2}-(D_{5,0}-C_{20})\frac{\partial^2 v_2}{\partial x^2}-\frac{1}{R^2}\left(\frac{D_{5,0}l^2}{4R^2}\right)\frac{\partial^2 v_2}{\partial\theta^2}\\
&-\frac{1}{R^2}(D_{2,0}+A_{20})\frac{\partial^2 v_2}{\partial\theta^2}+\frac{D_{5,0}l^2}{4R^2}\frac{\partial^4 v_2}{\partial x^2\partial\theta^2}+\frac{1}{R^2}\left(\frac{D_{5,0}l^2}{4R^2}+D_{4,0}k_s\right)v_2\\
&-\frac{D_{5,0}l^2}{4R}\frac{\partial^4 u_2}{\partial x^3\partial\theta}-\frac{D_{5,0}l^2}{4R^3}\frac{\partial^4 u_2}{\partial x\,\partial\theta^3}+\frac{1}{R}\left(\frac{D_{5,0}l^2}{4R^2}-D_{3,0}-D_{5,0}\right)\frac{\partial^2 u_2}{\partial x\,\partial\theta}\\
&+\frac{3D_{5,0}l^2}{4R^2}\frac{\partial^3 w_2}{\partial x^2\partial\theta}+\frac{D_{5,0}l^2}{4R^4}\frac{\partial^3 w_2}{\partial\theta^3}-\frac{1}{R^2}\left(D_{2,0}+\frac{D_{5,0}l^2}{4R^2}+D_{4,0}k_s\right)\frac{\partial w_2}{\partial\theta}\\
&-\frac{1}{R}\left(\frac{D_{5,0}l^2}{2R}+D_{5,1}+D_{3,1}+\frac{D_{5,1}l^2}{4R^2}\right)\frac{\partial^2\beta_{x2}}{\partial x\,\partial\theta}-\frac{1}{R^2}\left(\frac{D_{5,0}l^2}{4R}+D_{2,1}\right)\frac{\partial^2\beta_{\theta2}}{\partial\theta^2}\\
&-\left(\frac{3D_{5,0}l^2}{4R}+D_{5,1}+\frac{D_{5,1}l^2}{4R^2}\right)\frac{\partial^2\beta_{\theta2}}{\partial x^2}+\frac{D_{5,1}l^2}{4R^2}\frac{\partial^4\beta_{\theta2}}{\partial x^2\partial\theta^2}-\frac{D_{5,1}l^2}{4R^3}\frac{\partial^4\beta_{x2}}{\partial x\,\partial\theta^3}\\
&+\frac{D_{5,1}l^2}{4}\frac{\partial^4\beta_{\theta2}}{\partial x^4}-\frac{1}{R}\left(\frac{D_{5,0}l^2}{4R^2}+D_{4,0}k_s\right)\beta_{\theta2}-\frac{D_{5,1}l^2}{4R}\frac{\partial^4\beta_{x2}}{\partial x^3\partial\theta}\\
&-\frac{1}{R}\left(\frac{\partial N_{2,\varphi_0}}{\partial\theta}+\frac{\partial N_{2,\psi_0}}{\partial\theta}\right)-\frac{1}{R}\left(N_{2,\varphi}\frac{\partial\varphi_2}{\partial\theta}+N_{2,\psi}\frac{\partial\psi_2}{\partial\theta}\right)\\
&-\frac{1}{R}\left(-N_{4,\varphi}\frac{\partial\varphi_2}{\partial\theta}-N_{4,\psi}\frac{\partial\psi_2}{\partial\theta}\right)+I^{(1)}\frac{\partial^2\beta_{\theta2}}{\partial t^2}+I^{(0)}\frac{\partial^2 v_2}{\partial t^2}=0
\end{aligned}
\tag{C9}
$$

δw_2:

$$
\begin{aligned}
&\frac{D_{5,0}l^2}{4}\frac{\partial^4 w_2}{\partial x^4}-D_{5,0}(\frac{l^2}{4R^2}+k_s)\frac{\partial^2 w_2}{\partial x^2}+\frac{D_{5,0}l^2}{2R^2}\frac{\partial^4 w_2}{\partial x^2\partial\theta^2}+\frac{D_{5,0}l^2}{4R^4}\frac{\partial^4 w_2}{\partial\theta^4}\\
&-\frac{1}{R^2}(\frac{D_{5,0}l^2}{4R^2}+D_{4,0}k_s)\frac{\partial^2 w_2}{\partial\theta^2}+\frac{D_{2,0}}{R^2}w_2+\frac{D_{3,0}}{R}\frac{\partial u_2}{\partial x}+\frac{D_{5,0}l^2}{2R^3}\frac{\partial^3 u_2}{\partial x\partial\theta^2}\\
&-\frac{3D_{5,0}l^2}{4R^2}\frac{\partial^3 v_2}{\partial x^2\partial\theta}+\frac{1}{R^2}(D_{2,0}+\frac{D_{5,0}l^2}{4R^2}+D_{4,0}k_s)\frac{\partial v_2}{\partial\theta}-\frac{D_{5,0}l^2}{4R^4}\frac{\partial^3 v_2}{\partial\theta^3}\\
&-\frac{D_{5,0}l^2}{4R^2}\frac{\partial^3\beta_{x2}}{\partial x\partial\theta^2}-\frac{D_{5,0}l^2}{4}\frac{\partial^3\beta_{x2}}{\partial x^3}+(\frac{D_{5,0}l^2}{4R^2}-D_{5,0}k_s+\frac{D_{3,1}}{R})\frac{\partial\beta_{x2}}{\partial x}\\
&-\frac{D_{5,0}l^2}{4R^3}\frac{\partial^3\beta_{\theta2}}{\partial\theta^3}-\frac{1}{R}(\frac{D_{5,0}l^2}{4R^2}+D_{4,0}k_s-\frac{D_{2,1}}{R})\frac{\partial\beta_{\theta2}}{\partial\theta}\\
&-\frac{1}{2R}(\frac{D_{5,0}l^2}{2}+\frac{D_{5,1}l^2}{R})\frac{\partial^3\beta_{\theta2}}{\partial x^2\partial\theta}-\frac{1}{R}((\alpha_{11}\Delta T+\beta_{11}\Delta H)D_{3,0})\\
&-\frac{1}{R^2}(\alpha_{22}\Delta T+\beta_{22}\Delta H)D_{2,0})-\frac{1}{R}(-N_{2,\varphi_0}-N_{2,\varphi}\varphi_2-N_{2,\psi_0}-N_{2,\psi}\psi_2)\\
&+\frac{1}{R}N_{4,\varphi}\frac{\partial^2\varphi_2}{\partial\theta^2}+\frac{1}{R}N_{4,\psi}\frac{\partial^2\psi_2}{\partial\theta^2}+N_{5,\varphi}\frac{\partial^2\varphi_2}{\partial x^2}+N_{5,\psi}\frac{\partial^2\psi_2}{\partial x^2}+I^{(0)}\frac{\partial^2 w_2}{\partial t^2}\\
&-q(x,\theta)+K_{w2}(w_2-w_1)-K_{G2}\nabla^2(w_2-w_1)+K_{w3}w_2-K_{G3}\nabla^2 w_2=0
\end{aligned}
\tag{C10}
$$

$\delta\beta_{x2}$:

$$
\begin{aligned}
&-(\frac{D_{5,0}l^2}{4})\frac{\partial^2\beta_{x2}}{\partial x^2}-(D_{1,2}+A_{22})\frac{\partial^2\beta_{x2}}{\partial x^2}+\frac{D_{5,2}l^2}{4R^2}\frac{\partial^4\beta_{x2}}{\partial x^2\partial\theta^2}+\frac{D_{5,2}l^2}{4R^4}\frac{\partial^4\beta_{x2}}{\partial\theta^4}\\
&-\frac{1}{R^2}(D_{5,0}l^2-\frac{D_{5,1}l^2}{2R})\frac{\partial^2\beta_{x2}}{\partial\theta^2}-\frac{1}{R^2}(D_{5,2}+C_{22})\frac{\partial^2\beta_{x2}}{\partial\theta^2}+(\frac{D_{5,0}l^2}{4R^2})\beta_{x2}\\
&+(D_{5,0}k_s+C_{20})\beta_{x2}-\frac{1}{R}(-\frac{3D_{5,0}l^2}{4}+\frac{D_{5,1}l^2}{2R})\frac{\partial^2\beta_{\theta2}}{\partial x\partial\theta}\\
&-\frac{1}{R}(D_{3,2}+D_{5,2}+C_{22}+B_{22})\frac{\partial^2\beta_{\theta2}}{\partial x\partial\theta}-\frac{D_{5,2}l^2}{4R^3}\frac{\partial^4\beta_{\theta2}}{\partial x\partial\theta^3}-\frac{D_{5,2}l^2}{4R}\frac{\partial^4\beta_{\theta2}}{\partial x^3\partial\theta}\\
&+\frac{1}{R^2}(\frac{5D_{5,0}l^2}{4R})\frac{\partial^2 u_2}{\partial\theta^2}-\frac{1}{R^2}(D_{5,1}+C_{21})\frac{\partial^2 u_2}{\partial\theta^2}-\frac{1}{R}(\frac{D_{5,0}l^2}{2R}+\frac{D_{5,1}l^2}{4R^2})\frac{\partial^2 v_2}{\partial x\partial\theta}\\
&-\frac{1}{R}(+D_{3,1}+D_{5,1}+C_{21}+B_{21})\frac{\partial^2 v_2}{\partial x\partial\theta}+\frac{D_{5,0}l^2}{4}\frac{\partial^3 w_2}{\partial x^3}+\frac{D_{5,0}l^2}{4R^2}\frac{\partial^3 w_2}{\partial x\partial\theta^2}\\
&-(\frac{D_{5,0}l^2}{4R^2})\frac{\partial w_2}{\partial x}-(-D_{5,0}k_s+\frac{D_{3,1}}{R}-C_{20}+\frac{1}{R}B_{21})\frac{\partial w_2}{\partial x}-\frac{D_{5,1}l^2}{4R^3}\frac{\partial^4 v_2}{\partial x\partial\theta^3}\\
&-(D_{1,1}+A_{21})\frac{\partial^2 u_2}{\partial x^2}+\frac{D_{5,1}l^2}{4R^4}\frac{\partial^4 u_2}{\partial\theta^4}+\frac{D_{5,1}l^2}{4R^2}\frac{\partial^4 u_2}{\partial x^2\partial\theta^2}-\frac{D_{5,1}l^2}{4R}\frac{\partial^4 v_2}{\partial x^3\partial\theta}\\
&-\frac{\partial M_{1,\varphi_0}}{\partial x}-\frac{\partial M_{1,\psi_0}}{\partial x}-M_{1,\varphi}\frac{\partial\varphi_2}{\partial x}-M_{1,\psi}\frac{\partial\psi_2}{\partial x}-N_{5,\varphi}\frac{\partial\varphi_2}{\partial x}-N_{5,\psi}\frac{\partial\psi_2}{\partial x}\\
&+I^{(2)}\frac{\partial^2\beta_{x2}}{\partial t^2}+I^{(1)}\frac{\partial^2 u_2}{\partial t^2}=0
\end{aligned}
\tag{C11}
$$

$\delta\beta_{\theta2}$:

$$
\begin{aligned}
&\frac{D_{5,2}l^2}{4}\frac{\partial^4\beta_{\theta2}}{\partial x^4}-(D_{5,0}l^2+\frac{D_{5,2}l^2}{2R^2}+\frac{D_{5,1}l^2}{2R})\frac{\partial^2\beta_{\theta2}}{\partial x^2}-(D_{5,2}+C_{22})\frac{\partial^2\beta_{\theta2}}{\partial x^2}\\
&+\frac{D_{5,2}l^2}{4R^2}\frac{\partial^4\beta_{\theta2}}{\partial x^2\partial\theta^2}+\frac{D_{5,1}l^2}{4}\frac{\partial^4 v_2}{\partial x^4}-\frac{1}{R^2}(\frac{D_{5,0}l^2}{4})\frac{\partial^2\beta_{\theta2}}{\partial\theta^2}-\frac{1}{R^2}(D_{2,2}+A_{22})\frac{\partial^2\beta_{\theta2}}{\partial\theta^2}\\
&-\frac{1}{R}(-\frac{3D_{5,0}l^2}{4}+\frac{D_{5,1}l^2}{2R})\frac{\partial^2\beta_{x2}}{\partial x\partial\theta}-\frac{1}{R}(D_{3,2}+D_{5,2}+B_{22}+C_{22})\frac{\partial^2\beta_{x2}}{\partial x\partial\theta}\\
&-\frac{D_{5,1}l^2}{4R^3}\frac{\partial^4 u_2}{\partial x\partial\theta^3}-\frac{D_{5,2}l^2}{4R^3}\frac{\partial^4\beta_{x2}}{\partial x\partial\theta^3}-\frac{D_{5,2}l^2}{4R}\frac{\partial^4\beta_{x2}}{\partial x^3\partial\theta}-\frac{1}{R}(\frac{D_{5,0}l^2}{4R}-\frac{D_{5,1}l^2}{2R^2})\frac{\partial^2 u_2}{\partial x\partial\theta}\\
&-\frac{1}{R}(+D_{3,1}+D_{5,1}+B_{21}+C_{21})\frac{\partial^2 u_2}{\partial x\partial\theta}-(\frac{3D_{5,0}l^2}{4R}+\frac{D_{5,1}l^2}{4R^2})\frac{\partial^2 v_2}{\partial x^2}\\
&-(D_{5,1}+C_{21})\frac{\partial^2 v_2}{\partial x^2}-\frac{1}{R^2}(\frac{D_{5,0}l^2}{4R})\frac{\partial^2 v_2}{\partial\theta^2}-\frac{1}{R^2}(D_{2,1}+A_{21})\frac{\partial^2 v_2}{\partial\theta^2}-\frac{1}{R}(\frac{D_{5,0}l^2}{4R^2})v_2\\
&-\frac{1}{R}(C_{20}+k_sD_{4,0})v_2+\frac{1}{R}(\frac{D_{5,0}l^2}{4}+\frac{D_{5,1}l^2}{2R})\frac{\partial^3 w_2}{\partial x^2\partial\theta}+\frac{D_{5,0}l^2}{4R^3}\frac{\partial^3 w_2}{\partial\theta^3}\\
&+\frac{1}{R}(\frac{D_{5,0}l^2}{4R^2})\frac{\partial w_2}{\partial\theta}+\frac{1}{R}(+k_sD_{4,0}-\frac{D_{2,1}}{R}+C_{20}-\frac{A_{2,1}}{R})\frac{\partial w_2}{\partial\theta}+\frac{D_{5,1}l^2}{4R^2}\frac{\partial^4 v_2}{\partial x^2\partial\theta^2}\\
&-\frac{D_{5,1}l^2}{4R}\frac{\partial^4 u_2}{\partial x^3\partial\theta}+(\frac{D_{5,0}l^2}{4R^2})\beta_{\theta2}+(k_sD_{4,0}+C_{20})\beta_{\theta2}-\frac{1}{R}(\frac{\partial M_{2,\varphi_0}}{\partial\theta}+\frac{\partial M_{2,\psi_0}}{\partial\theta})\\
&-\frac{1}{R}M_{2,\varphi}\frac{\partial\varphi_2}{\partial\theta}-\frac{1}{R}M_{2,\psi}\frac{\partial\psi_2}{\partial\theta}-N_{4,\varphi}\frac{\partial\varphi_2}{\partial\theta}-N_{4,\psi}\frac{\partial\psi_2}{\partial\theta}+I^{(1)}\frac{\partial^2 v_2}{\partial t^2}+I^{(2)}\frac{\partial^2\beta_{\theta2}}{\partial t^2}=0
\end{aligned}
\tag{C12}
$$

$\delta\varphi_2$:

$$\begin{aligned}&N_{5,\varphi}\left(\frac{\partial^2 w_2}{\partial x^2}+\frac{\partial\beta_{x2}}{\partial x}\right)+N_{1,D}\frac{\partial^2\varphi_2}{\partial x^2}+N_{1,B}\frac{\partial^2\psi_2}{\partial x^2}+N_{4,\varphi}\left(\frac{1}{R}\frac{\partial^2 w_2}{\partial\theta^2}+\frac{\partial\beta_{\theta2}}{\partial\theta}-\frac{1}{R}\frac{\partial v_2}{\partial\theta}\right)\\&+N_{2,B}\frac{\partial^2\varphi_2}{\partial\theta^2}+N_{2,D}\frac{\partial^2\psi_2}{\partial\theta^2}+N_{1,\varphi}\frac{\partial u_2}{\partial x}+M_{1,\varphi}\frac{\partial\beta_{x2}}{\partial x}+\frac{1}{R}N_{2,\varphi}\left(w_2+\frac{\partial v_2}{\partial\theta}\right)+M_{2,\varphi}\frac{\partial\beta_{\theta2}}{\partial\theta}\\&-N_{3,D1}\varphi_0-N_{3,D}\varphi_2-N_{3,B1}\varphi_0-N_{3,B}\varphi_2=0\end{aligned}\tag{C13}$$

$\delta\psi_2$:

$$\begin{aligned}&N_{5,\psi}\left(\frac{\partial^2 w_2}{\partial x^2}+\frac{\partial\beta_{x2}}{\partial x}\right)+N_{1,B}\frac{\partial^2\varphi_2}{\partial x^2}+N_{1,B1}\frac{\partial^2\psi_2}{\partial x^2}+N_{4,\psi}\left(\frac{1}{R}\frac{\partial^2 w_2}{\partial\theta^2}+\frac{\partial\beta_{\theta2}}{\partial\theta}-\frac{1}{R}\frac{\partial v_2}{\partial\theta}\right)\\&+N_{2,D}\frac{\partial^2\varphi_2}{\partial\theta^2}+N_{2,B1}\frac{\partial^2\psi_2}{\partial\theta^2}+N_{1,\psi}\frac{\partial u_2}{\partial x}+M_{1,\psi}\frac{\partial\beta_{x2}}{\partial x}+\frac{1}{R}N_{2,\psi}\left(w_2+\frac{\partial v_2}{\partial\theta}\right)+M_{2,\psi}\frac{\partial\beta_{\theta2}}{\partial\theta}\\&-N_{3,B1}\varphi_0-N_{3,B}\varphi_2-N_{3,D2}\psi_0-N_{3,B2}\psi_2=0\end{aligned}\tag{C14}$$